

Computational Fluid Dynamics (CFD) Models

C. Mingham, L. Qian, D. Causon

School of Computing, Mathematics and Digital Technology, Manchester Metropolitan University,
Manchester, England

6.1 INTRODUCTION AND FUNDAMENTAL PRINCIPLES

As computers have become ever more powerful, the discipline of computational fluid dynamics (CFD) has become an increasingly viable numerical approach for simulating the dynamic behaviour of wave energy converters (WECs). In theory, CFD can be used to study the design of a particular WEC, conduct parametric studies to optimize its performance and investigate wave loadings to characterize its survivability in extreme seas. Given enough computing power CFD could also simulate the performance of arrays of WECs. However, the construction and application of suitable CFD models remains challenging, with many issues needing to be resolved for them to reach their full potential.

In CFD the underlying physical laws describing fluid flow (eg, conservation of mass, momentum, etc.) are expressed mathematically as a system of partial differential equations (PDEs). Classically, these equations are the well-known Navier–Stokes equations together with the continuity equation (Drazin and Riley, 2006). To complete the mathematical model, initial conditions are given together with

the internal and external boundary conditions needed to define the WEC geometry, the bathymetry and the wave field. In general, the describing system of PDEs cannot be solved analytically so approximate solutions are obtained via numerical algorithms (called solvers) implemented on digital computers. These solutions are the values of the relevant dependent variables (eg, pressure, velocity, etc.) at discrete spatial points in the computational domain and at discrete times as the simulation progresses. In principle, solutions can be found to any specified degree of accuracy at specified points in space and time; however, in reality their formal accuracy depends on the underlying numerical algorithm or discretization scheme.

CFD methods can be separated broadly into two categories: Eulerian and Lagrangian. In the Eulerian approach the computational domain is discretized by a finite set of points called a grid (or mesh) and the approximate solution is computed at these grid points. These approximations can be carried out in several different ways depending on the underlying mathematical theory. Two popular approaches are the finite difference method and the finite volume method. The finite difference method is based on Taylor

theory to approximate partial derivatives at the grid points. An introduction to the finite difference method can be found in [Causon and Mingham \(2010\)](#) or in [Leveque \(2007\)](#). The finite volume method uses the Gauss divergence theorem to express spatial partial derivatives as surface integrals. In the finite volume method the spatial grid is viewed as a set of cells and the approximate numerical solutions are usually but not necessarily computed at the centroid of each cell. An introduction to the finite volume method can be found in [Causon et al. \(2011\)](#) or in [Versteeg and Malalasekera \(2007\)](#). The majority of Eulerian CFD methods applied to WEC simulation are based on the finite volume method because of its geometric flexibility and physically consistent treatment of the flow across cell boundaries.

In the Lagrangian approach the computational region is discretized by a set of particles which move at the local flow velocity and approximate solutions are computed at the position of each particle at each discrete time. Amongst several Lagrangian methods the smoothed-particle hydrodynamics (SPH) method in its various forms is becoming popular, although it is not yet a mature technology.

A CFD approach has several potential advantages over the physical modelling of WECs in wave tanks:

- CFD models are relatively cheap to set up,
- the WEC geometry and wave conditions can be changed easily,
- CFD models do not normally suffer from scaling problems and
- data can be obtained at any points of interest in the computational domain.

Conversely, it should also be noted that CFD models have some disadvantages compared to physical tank models:

- run times are typically much slower than for the execution of a tank test
- if an inappropriate CFD model is used, the model may not capture all of the relevant physics correctly

- the approximating algorithms may introduce large errors in the numerical solutions.

CFD code is often used in the form of a so-called numerical wave tank (NWT) to simulate a WEC. A NWT is a CFD model that includes not only the WEC itself, but also the boundaries defining the dimensions of the surrounding water. However, the construction of a WEC in an NWT is a nontrivial task. Even with a prewritten code, significant expertise is generally needed to produce useful results and there are certain fundamental questions to be answered before running a CFD simulation. The most important question to ask is 'Does the CFD model capture all of the relevant physics of the situation to be simulated?', ie, do the underlying equations describe all the important physical processes that will occur? No CFD model can capture every aspect of the physics and decisions have to be made as to what physics to model and what physics to ignore. Then, before running the required simulations, the CFD model must be *validated* by comparing numerical results to those from a physical model, usually via a wave tank or field data. Validation must be done for tests involving the physical processes that are to be ultimately simulated. This is not an easy task since it is usually difficult to ensure that physical and computational boundary conditions match exactly, so some degree of difference in the compared results must be accepted even if the CFD model includes all of the relevant physics. A second important question is 'Have the numerical algorithms been coded correctly?', ie, is the code doing what it is supposed to do? This is the issue of *verification*. Ideally, all branches of the code should be rigorously tested for coding accuracy via small test problems with known output data. However, this is inevitably time consuming as there are often thousands of lines of code; moreover, this is impossible if the user of the CFD package does not have access to the source code. In such cases, the best that can be done is to compare the results to other independent CFD codes over a range of situations and to use known analytical solutions for simpler test cases.

It should be noted that numerical algorithms, even if correctly coded, contain intrinsic errors due to the numerical approximations to the derivatives referred to earlier, so it is important to extend the verification process to check that the algorithms do not produce excessive numerical dissipation or diffusion. Only after a CFD code has been validated and verified should it be used for WEC simulations. A final fundamental step in obtaining reliable simulation results addresses the issue of convergence. Errors are introduced by the spatial discretization so it is desirable to demonstrate that results are independent of the computational grid. Any simulation should be repeated on finer grids until corresponding results on successive grids are within some specified tolerance. In this way a grid converged solution is obtained.

6.2 INCOMPRESSIBLE CFD MODELS

The most common type of CFD model used for modelling WECs is based on an incompressible representation of the Navier–Stokes equations. Within this type of CFD model the WEC engineer has a large number of CFD modelling tools from which to choose. Some of these modelling tools are freely available, including source code, while others are commercial ‘black box’ packages available often under license. Without exception, significant expertise is needed both to select the appropriate model and then to set up and run a simulation. Generally speaking, commercial packages come with user support and are well documented and are easier to use than the open-source CFD models so may be the best choice for the WEC engineer who wants results quickly. However, some commercial packages do not use the most up-to-date solver algorithms, giving rise to unnecessary numerical errors; it has been the authors’ experience that some commercial packages that purport to be able to simulate fully 3D WEC dynamics do not even simulate a simple wave field correctly (although promotional literature may include enticing images of devices in

waves!). All models have their limitations and the choice of model should be informed by the important physics in the WEC simulation. The following is a nonexhaustive list of some commercial CFD packages that have been used for WEC simulation:

- ANSYS Fluent,
- CFX,
- FLOW-3D and
- Star-CD/CCM+.

Some of the free open-source or in-house CFD codes that have been used to model WECs are:

- AMAZON,
- Code-Saturne,
- ComFLOW and
- OpenFoam (more on this package later).

A relatively large number of CFD models of oscillating water columns (OWCs) have been developed. [Alves and Sarmiento \(2006\)](#) used a two-dimensional CFD package and investigated vortex shedding at the OWC’s front lip, wave impacts on the front and back walls and sloshing inside the chamber. Although the results do not appear to be compared to any experimental data, the results appear to be qualitatively reasonable and it is claimed that the CFD model is suitable for investigating these hydrodynamics. [Zhang et al. \(2012\)](#) and [Luo et al. \(2014\)](#) also developed two-dimensional models of OWCs and compared their results to experimental data. Typically they found that the results of a CFD model compared better to experimental results than those based on linear potential flow theory, especially for larger waves. The authors also developed a model of an OWC ([Qian et al., 2005](#)), which is discussed in more detail following.

An early example of a CFD model with a moving WEC was produced by [Agamloh et al. \(2008\)](#), who modelled an isolated and a pair of heaving buoys in three dimensions using the COMET CFD package. The response and power capture are calculated from the motion of the buoys, which although not compared to experiment or other theory do show an expected

decrease in conversion efficiency with wave amplitude. Other examples of CFD models of moving WECs include the SEAREV WEC (Babarit et al., 2009), an oscillating wave surge converter (Schmitt et al., 2012; Henry et al., 2014), a moored heaving WEC (Palm et al., 2013), a two-body heaving WEC (Yu and Li, 2013), and a heaving/surging horizontal cylinder (Anbarsooz et al., 2014). As with the OWC models, it was typically found that the CFD models produced better estimates of the hydrodynamic forces than linear potential flow models, although the modelled responses were still often noticeably different to the measured responses of wave-tank models of the WECs.

In addition, a comparison of several commercial and noncommercial CFD codes, including SPH models, applied to the Pelamis and Manchester Bobber WECs, is presented in Westphalen et al. (2009) and a review of the CFD modelling of WECs is provided by Wolgamot and Fitzgerald (2015).

Rather than detail the attributes of the various competing CFD codes, which could quickly become out-of-date, some general observations on what features are desirable in a code are presented. In addition, as way of illustration, the features of the authors' own AMAZON suite of in-house codes are described in more detail and some of their results presented.

Most WECs operate in two fluids, namely air and water. Furthermore waves are likely to *break* in shallow water and/or storm conditions. WEC simulations have been carried out using *single* fluid CFD solvers where the numerical solution is computed only in the water component and the air/water interface (ie, the free surface) is found via a surface boundary condition. This approach breaks down or gives the wrong solutions when water heights become multivalued under wave breaking. More useful are *two-fluid* solvers where the underlying fluid equations are solved simultaneously in both air and water components. This is a numerically challenging task because of the large discontinuity in density across the air/water interface (water being a

thousand times denser than air). The volume of fluid (VoF) method (see, eg, Ubbink, 1997) is one way of obtaining the air/water interface. Essentially at each time step the volume fraction, F , of water in each computational cell ($F=0$ means that the cell contains only air, $F=1$ means that the cell contains only water) is calculated and regarded as a transported flow variable which satisfies a local advection equation. The F values are found at the new time level by solving the advection equation and the new interface is reconstructed from local F values. The VoF method can handle breaking waves although reconstruction of the interface becomes complicated in 3D.

A quite different method, used by the authors, is to capture the air/water interface *automatically* as the numerical solution proceeds in a manner similar to shock capturing in aerodynamics (Qian et al., 2006). In this approach the fluid density, ρ (which for an incompressible model is constant in each fluid), is treated as a variable and solved for throughout the computational region along with the other flow variables such as pressure and velocity. A modern Riemann-based approach is used together with appropriate flux limiters to suppress oscillations caused by large spatial gradients. For visualization purposes the air/water interface is determined by contour values where $\rho=500 \text{ kg/m}^3$. This method handles wave breaking naturally but care must be taken to use an appropriate high resolution method to avoid unnecessary numerical errors. In the authors' incompressible finite volume AMAZON-SC code the air/water interface is sharply defined being spread over a couple of computational cells due to unavoidable numerical diffusion. The inviscid form of the AMAZON-SC model and the basic underlying equations are,

$$\frac{\partial \mathbf{U}}{\partial t} + \frac{\partial \mathbf{F}_1}{\partial x} + \frac{\partial \mathbf{F}_2}{\partial y} + \frac{\partial \mathbf{F}_3}{\partial z} = \mathbf{B} \quad (6.1a)$$

where \mathbf{U} is a column matrix of conserved variables, \mathbf{F}_i are column matrices containing flux terms and \mathbf{B} is a column matrix of source terms. \mathbf{U} , \mathbf{F}_i and \mathbf{B} are given by,

$$\mathbf{U} = [\rho, \rho u, \rho v, \rho w, p]^T \quad (6.1b)$$

$$\mathbf{F}_1 = [\rho u, \rho u^2 + p, \rho uv, \rho uw, u]^T \quad (6.1c)$$

$$\mathbf{F}_2 = [\rho v, \rho uv, \rho v^2 + p, \rho vw, v]^T \quad (6.1d)$$

$$\mathbf{F}_3 = [\rho w, \rho uw, \rho vw, \rho w^2 + p, w]^T \quad (6.1e)$$

$$\mathbf{B} = [0, 0, -\rho g, 0, 0]^T \quad (6.1f)$$

and $p = p(x, y, z)$ is pressure, $\rho = \rho(x, y, z)$ is density and u, v , and w are the components of the flow velocity in x, y and z directions, respectively. Note that these equations are actually rewritten in integral form for the finite volume approach used in AMAZON-SC but we present them here in differential form for ease of comparison with the related compressible two-phase model in Section 6.3. Viscous effects including suitable turbulence models, where these are available, can be included easily via additional source terms.

Details of the incompressible surface capturing method applied to a WEC simulation can be found in Qian et al. (2005). AMAZON-SC simulations of a scaled cross-section of the LIMPET OWC (Fig. 6.1) and an oscillating wave surge converter (Fig. 6.2) are given in the following paragraphs.

In Fig. 6.1, the free surface patterns and velocity vectors in both water and air around a scaled LIMPET WEC model are shown at four typical instants during one period of the flow development. Regular waves with a wave length of 1.5 m were generated by a moving paddle located at the left-hand side of the NWT. The boundary surface contours of the device itself are represented by the Cartesian cut cell method which represents these accurately (see the following). As the wave front interacts with the device it drives the water column inside the chamber to move up and down with the same period as the waves, but with a slightly different phase. A jet of air is clearly seen to be alternately driven out of the chamber and sucked into it due to the motion of the OWC.

An oscillating wave surge converter, consisting of an oscillating vane which responds to the predominant and amplified horizontal fluid motion in shallow and intermediate depth waves, has also been simulated under regular waves. The angular velocity of the vane is derived from the motion of the waves, ie, by calculating the torque from the pressure exerted on its surface. Several snapshots showing the wave profiles and velocity vectors around the device are presented in Fig. 6.2. This test case clearly demonstrates the potential of CFD to deal with complex wave/paddle interactions and real fluid flow problems.

A second important feature of a CFD NWT code for simulating WECs is the ability to deal with the motion of the device correctly. Typically WECs have 6 degrees-of-freedom and the motion may be extreme in storm conditions. Grid generation has a key role to play here. One gridding approach is to stretch and compress the grid locally around the WEC as it moves in order to ensure that the grid remains body fitted at all times (Bhinder et al., 2009, 2011). This approach is efficient for small amplitude oscillatory motion of the WEC but breaks down, or needs frequent remeshing, in violent wave conditions when the device motion becomes large and grid cells become highly skewed. Another approach is to embed the WEC in its own interior body fitted subgrid which moves with the WEC without changing its topology within a fixed external grid (Schmitt and Elsaesser, 2015). At each time step a procedure is used to interpolate the data at the intersection of the sub grid and the fixed external grid. Such a gridding strategy can, in principle, cope with arbitrary WEC motion although there remains the problem of generating a suitable body fitted internal grid and the data interpolation at the interior and exterior grid boundaries must be done with care.

The authors have used another gridding approach within their AMAZON suite of codes. This approach is the Cartesian cut cell method (Causon et al., 2001). In 2D the computational domain is overlaid with a simple Cartesian grid.

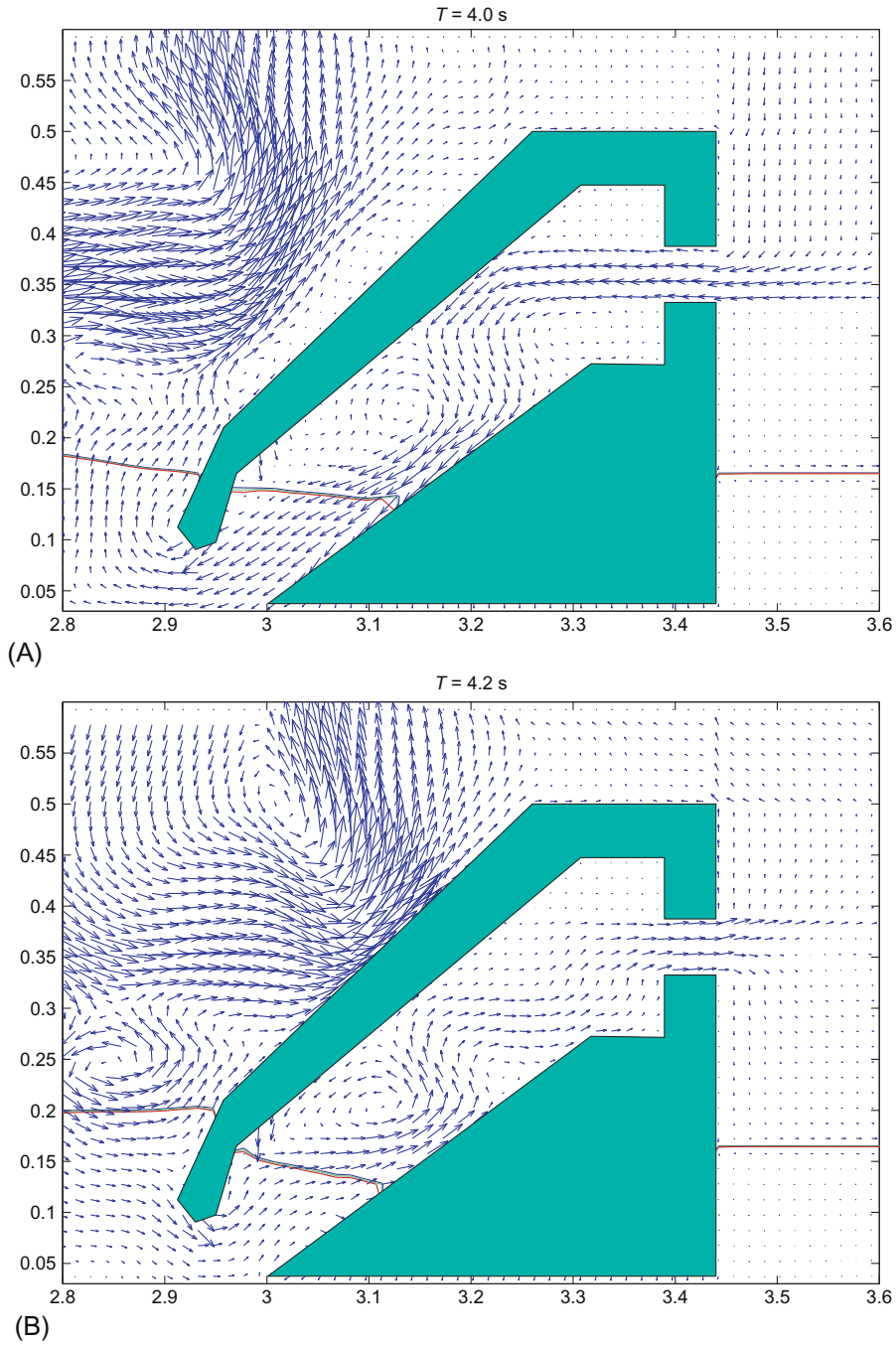


FIG. 6.1 AMAZON-SC simulation of the LIMPET WEC showing velocity vectors in air and water at different times (A: $T=4.0$ s, B: $T=4.2$ s, C: $T=4.4$ s and D: $T=4.6$ s).

(Continued)

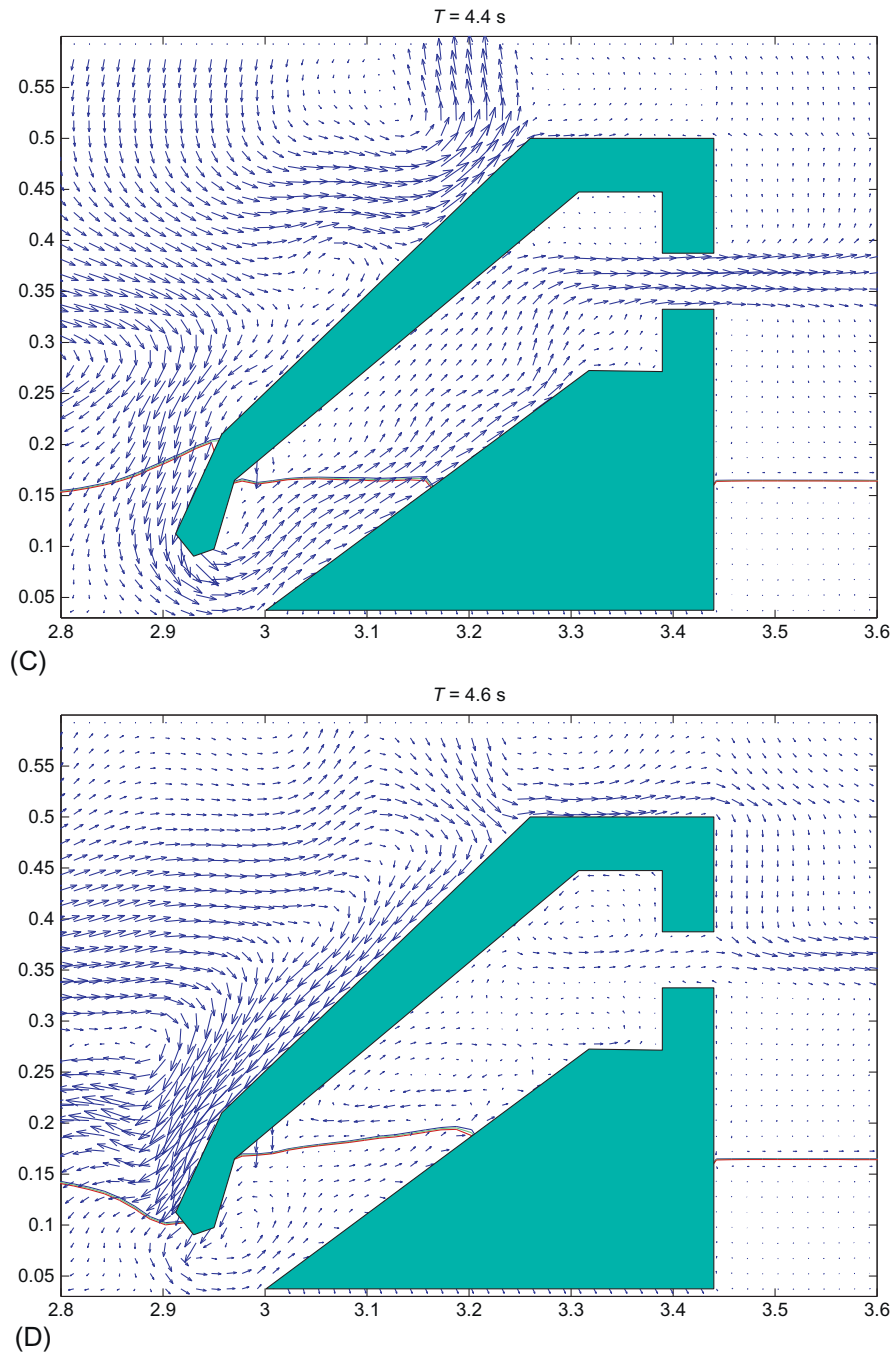


FIG. 6.1, CONT'D

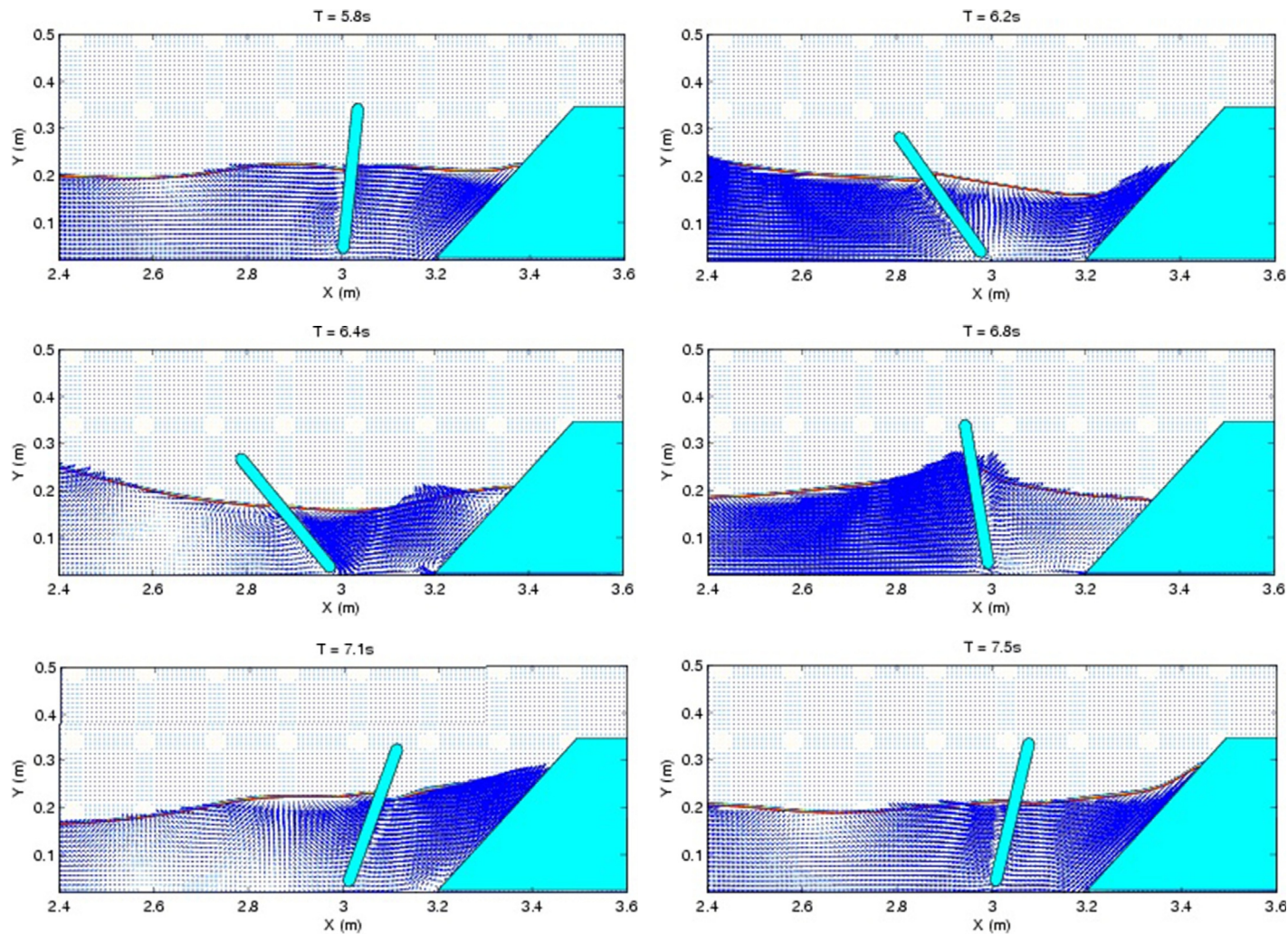


FIG. 6.2 AMAZON-SC simulation of an oscillating wave surge converter showing velocity vectors in the water at different times as the paddle oscillates.

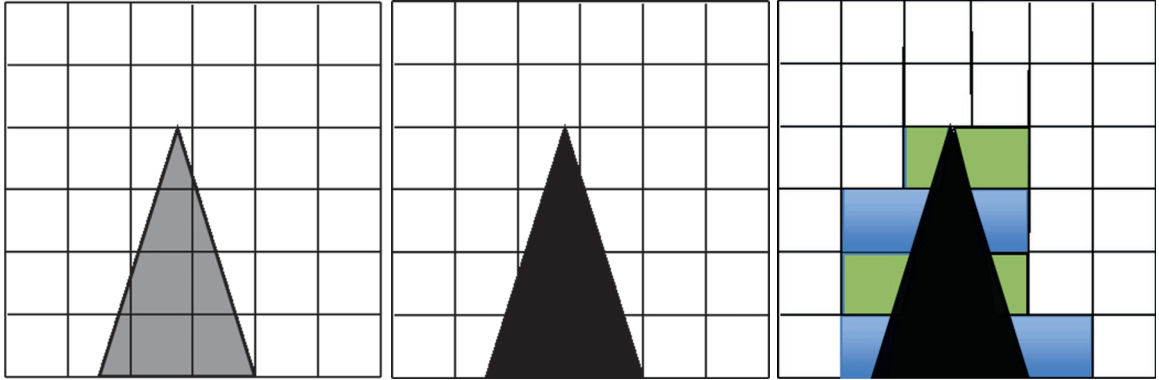


FIG. 6.3 Cartesian cut cell grid generation. *Left*: Solid body and background Cartesian grid. *Middle*: Unmerged cut cells around solid body. *Right*: Cut and merged cells shown as *shaded*.

The intersections of the grid with any irregular external and internal (ie, the WEC) solid boundaries are computed and the affected grid cells are *cut* so as to produce a body fitted grid in which cut cells have five or more sides (small 3-sided cells being merged with larger neighbouring cells) whilst the majority of cells remain rectangular Cartesian. Fig. 6.3 shows the basic idea of the cut cell method.

Moving boundaries are treated by simply recomputing cell cuts as the body moves through the background regular Cartesian grid for as long as the motion continues so that the computational grid remains boundary fitted at all times. This process is computationally efficient and, once the solid boundaries in the computational domain are specified, grid generation is automatic and no special user expertise is needed. The Cartesian cut cell method extends naturally to 3D (Yang et al., 2000). AMAZON simulations for a 3D Bobber type WEC undergoing free fall motion are presented in Hu et al. (2011).

6.3 COMPRESSIBLE TWO-PHASE CFD MODELS

Historically most CFD simulations of WECs have been based on *incompressible* models for the air and water components and this is true

of the AMAZON results given previously (note that AMAZON-SC is a two-fluid model and each fluid is treated as incompressible and cannot undergo phase change). The assumption of incompressibility is valid in many cases as water is difficult to compress and the air above the free surface does not affect the WEC dynamics appreciably. However, compressibility effects may be significant when considering WEC survivability in storm conditions. Violent wave interaction with WECs produces a variety of complex physical phenomena. Air bubbles may be entrained into the surrounding water and air pockets may be trapped against the WEC during wave interaction. Aerated water behaves very differently to pure water due to its increased compressibility. The sound speed in aerated water drops quickly (from 1500 m s^{-1} for pure water to less than 100 m s^{-1} at only 5% aeration) with aeration level leading to the possibility of transonic shock wave and rarefaction phenomena even at the relatively low particle velocities occurring at wave impact. Large fluctuations of pressure within trapped air pockets can also occur. Pressures may drop so low due to rapid local air pocket expansion that the surrounding water evaporates (and then recondenses once the air pressure rises again). Clearly

incompressible codes cannot capture these physical processes, nor even those that treat the air component as compressible and the water component as incompressible. It should also be noted that physical tank tests are difficult to perform with aerated water due to difficulties in generating and controlling aeration levels and measuring particle velocities and pressures in a bubbly environment. Such physical models are also often intrinsically unscalable due to the different scaling laws that apply for air and water, and this is a good reason for using CFD where this problem does not generally occur.

It may be thought that, since the cushioning effect of compressible air and aerated water will reduce violent wave loadings on WECs, incompressible codes would still be useful for survivability calculations as they would tend to overestimate loadings, especially for single fluid-based solvers. However, there are two problems with this view. First, because the incompressible assumption, especially for

the water phase, does not capture the correct physics these codes can produce spurious results and can significantly *underestimate* impact pressures. This has been demonstrated conclusively by comparing the impact pressures generated by a range of incompressible and compressible codes for the benchmark test case of the free drop of a water column and its impact onto a 2D tank floor (Fig. 6.4, Ma et al., 2014). Secondly, the complex physics produced by compressible fluids could potentially give rise to further *increased* impact pressure in cases where reflected shocks combine or focus. The associated physics is currently not well understood and is a subject of ongoing research.

Clearly, more sophisticated CFD models are required and the authors have extended their incompressible in-house code AMAZON-SC CFD model to AMAZON-CW, in which both water and air components are treated as compressible fluids and the water can change phase in response to large local pressure variations

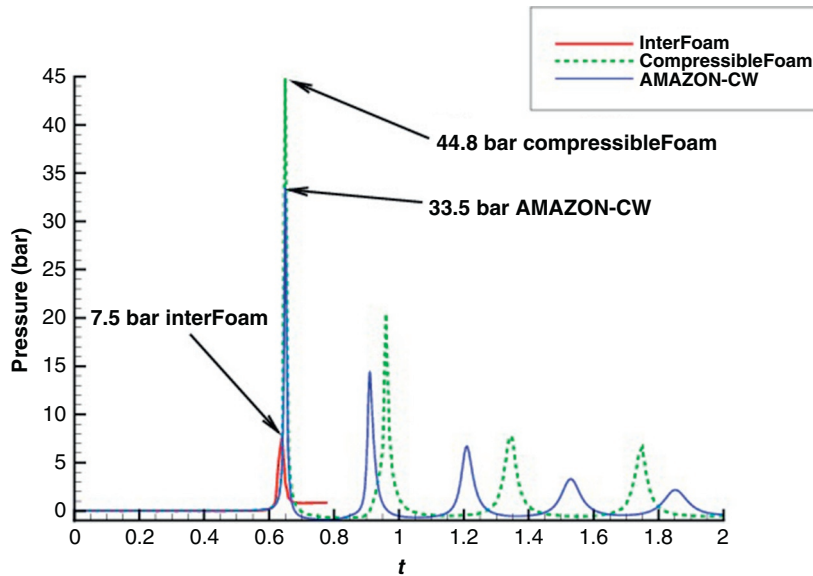


FIG. 6.4 Comparison of impact pressures from incompressible and compressible CFD codes showing time histories of impact pressures at the centre of the tank floor.

(Ma et al., 2014). The basic equations extended from those of Eqs (6.1) are

$$\frac{\partial \mathbf{U}}{\partial t} + \frac{\partial \mathbf{F}_1}{\partial x} + \frac{\partial \mathbf{F}_2}{\partial y} + \frac{\partial \mathbf{F}_3}{\partial z} = \mathbf{B} \quad (6.2a)$$

$$\mathbf{U} = [\alpha_1 \rho_1, \alpha_2 \rho_2, \rho u, \rho v, \rho w, \rho e]^T \quad (6.2b)$$

$$\mathbf{F}_1 = [\alpha_1 \rho_1 u, \alpha_2 \rho_2 u, \rho u^2 + p, \rho uv, \rho uw, \rho hu]^T \quad (6.2c)$$

$$\mathbf{F}_2 = [\alpha_1 \rho_1 v, \alpha_2 \rho_2 v, \rho uv, \rho v^2 + p, \rho vw, \rho hv]^T \quad (6.2d)$$

$$\mathbf{F}_3 = [\alpha_1 \rho_1 w, \alpha_2 \rho_2 w, \rho uw, \rho vw, \rho w^2 + p, \rho hw]^T \quad (6.2e)$$

$$\mathbf{B} = [0, 0, 0, -\rho g, 0, -\rho g v]^T \quad (6.2f)$$

where the variables are defined as in Eqs (6.1) and e is energy, ρ_i is the density of fluid i ($i=1$ indicates air, $i=2$ indicates water), α_i is the volume fraction of fluid i in a cell and h is the enthalpy, given by

$$h = (\rho e + p)/\rho \quad (6.2g)$$

The underlying flow model treats the dispersed water wave as a compressible mixture of air and water with homogeneous material properties. The corresponding mathematical equations are based on a multiphase flow model which builds on the conservation laws of mass, momentum and energy as well as the gas-phase volume fraction advection equation. A high-order finite volume scheme based on monotone upstream-centred schemes for conservation law (MUSCL) reconstruction is used to discretize the integral form of the governing equations. The numerical flux across a mesh cell face is estimated by means of the HLLC approximate Riemann solver. A third-order total variation diminishing Runge-Kutta scheme is adopted to obtain a time-accurate solution. The present model provides an effective way to deal with the compressibility of air and

water-air mixtures. Several test cases have been calculated using the present approach, including a gravity-induced liquid piston, free drop of a water column in a closed tank, water-air shock tubes, slamming of a flat plate into still pure and aerated water and a plunging wave impact at a vertical wall. The obtained results agree well with experiments, exact solutions and other numerical computations (Ma et al., 2014). Furthermore, the results illustrate through compressible simulations that during a violent wave impact a vertical wall may be subject to both positive and negative loading as shown in Fig. 6.5. This demonstrates the potential of the current method to tackle more general violent wave-air-structure interaction problems, including the simulation of extreme wave loads on WEC devices.

6.4 SMOOTHED-PARTICLE HYDRODYNAMIC MODELS

Although SPH was originally developed in the 1970s (for astrophysical problems), it is only recently that it has been used in the modelling of WECs. SPH models essentially represent the fluid as a mass of interacting particles, where the interaction between the particles and boundaries is dictated by the governing hydrodynamics. Together with this, smoothing kernels are applied to the calculated properties between the locations of the particles. A range of different methods of constructing and solving SPH models has been developed, whose discussion is beyond the scope of this book; further information can be obtained in Monaghan (2012). SPH models have a number of advantages over the more traditional CFD models described above including automatic conservation of mass and a simplification of surface-tracking, as the free surface is simply the boundary between the existence (water) and nonexistence (air) of particles. This makes SPH particularly suitable for extreme wave events with wave breaking.

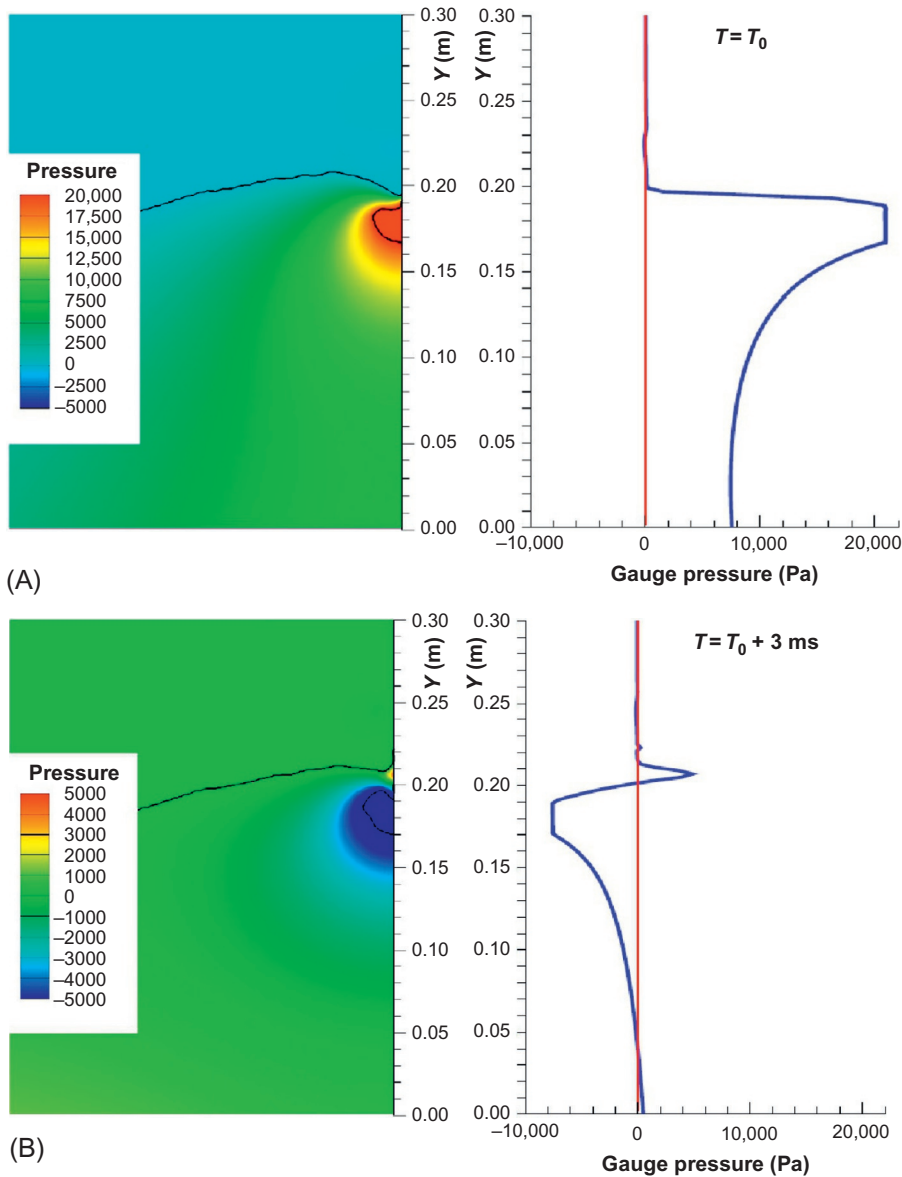


FIG. 6.5 Compressible CFD model simulation of violent impact loads on a vertical wall at two different times (A: $T = T_0$ and B: $T = T_0 + 3 \text{ ms}$).

The relatively recent application of SPH to WECs means that there are limited examples of its application. The first known application of SPH to a WEC is the application to SEACAP (Thilleul et al., 2011), which involved simulating

an extreme 35-m high wave event and calculating the expected pressures and loads. A second application of SPH to a WEC is the simulation of a heaving buoy in extreme waves, where an extreme wave event was represented using the

focused wave group, NewWave (Omidvar et al., 2012). The SPH simulations were compared to wave-tank experiments where it was found that, although the buoy motions before and after the wave group focus were not well modelled, the peak response was replicated relatively well. An example of the application of SPH to a non-extreme event is the modelling of a flap-type WEC (Rafiee et al., 2013). These results were again compared to wave-tank experiments where it was found that the SPH model produced estimates of the flap rotation and pressure in reasonable agreement with the wave-tank results.

6.5 LIMITATIONS

In general WEC dynamics involves complex physical processes which present severe challenges for CFD modelling. It is only by honestly acknowledging the limitations of CFD models and solvers that progress can be made in WEC simulation. One practical limitation of CFD at the present time is computational speed. Ideally WEC engineers would like to be able to run parametric studies with 3D models on desk top computers and obtain useful results in minutes or perhaps a few hours at most. This would allow WEC designs to be modified and their performance to be optimized over a range of wave climates. However, at the present time 3D simulations typically take hours, days (or even weeks!) depending on the case being studied. The authors' AMAZON-SC incompressible code, although based on modern solver technology, uses time steps of the order of microseconds (for numerical stability) and is therefore impractical for simulations of more than a few seconds of real time. This can be unfavourably compared to the typical duration of a storm (3 h or 10,800 s), which is often required to be modelled to ensure that all the potential extreme events and loads are included. Compressible models require similar resources.

The grid generation procedure can be another limitation on compute speed and solution accuracy. A fine grid is needed around the WEC to render its geometry accurately and at the free surface to capture the air/water interface. Coarser grid cells can be used away from these regions. A balance must be achieved between solution accuracy from a fine grid and compute speed from a coarse grid. However, this is further complicated by the dynamics of the WEC. If a locally body fitted grid moves in response to large amplitude WEC motion, then cells may become stretched so much that the simulation breaks down. If an overlapping block grid approach is used, then the necessary interpolation of data between small and large cells could produce unacceptable errors in the solution.

Another limitation arises from the numerics. Approximate solutions to the CFD model are obtained from algorithms derived from discretizations of the underlying continuous equations. To a greater or lesser degree these algorithms give rise to intrinsic and unavoidable numerical dissipation and/or dispersion which degrade solutions, particularly over long simulations. We have observed linear waves reduce greatly in amplitude as they cross a NWT due to numerical dissipation (and this was from an expensive commercial CFD package!). Yet another limitation arises when considering peak impact pressures. Pressure peaks occur over short time scales and seem to be very sensitive to cell size. It is important to use small time steps to capture or sample the pressure peak accurately but this can give excessively long run times. We have also found that it is necessary to use a fine mesh to obtain a mesh-converged solution when considering peak pressures and this is illustrated in Fig. 6.6, which shows time series of pressure for a water column falling onto a tank floor using the AMAZON-CW code on successively finer grids. This topic is of great current interest to the CFD wave/structure interaction (WSI) community and research into this area is ongoing.

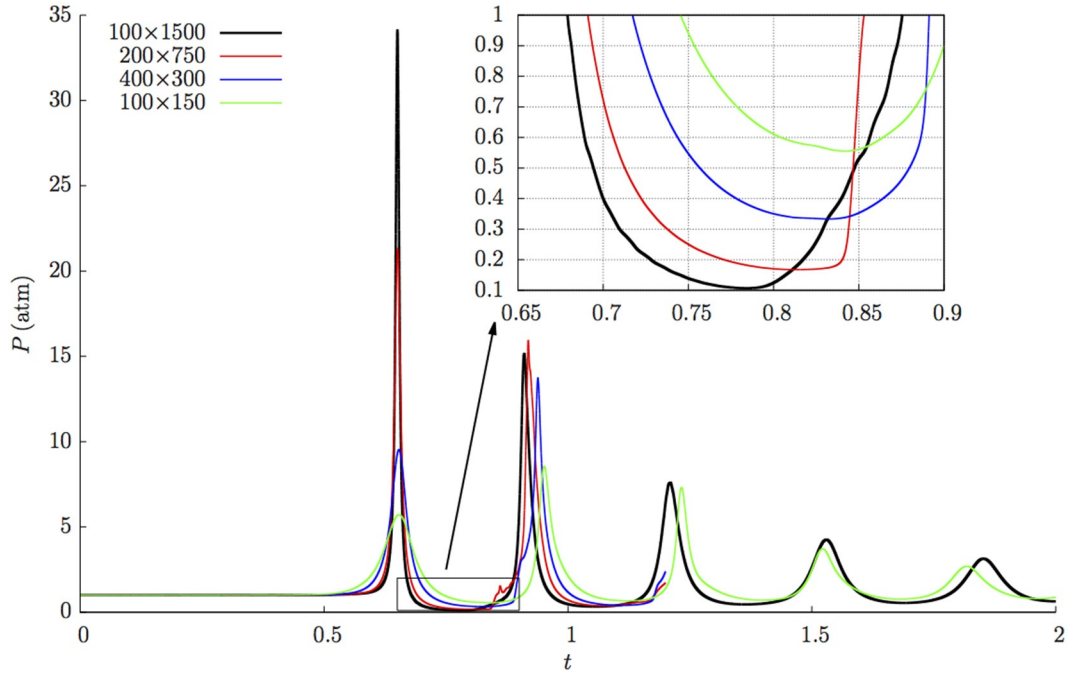


FIG. 6.6 AMAZON-CW solutions for peak pressure for different grid sizes for a water column falling onto a solid floor.

The previously stated limitations are essentially dependent on the flow solver. More fundamental limitations come from the model itself, which necessarily contains assumptions and approximations. It is assumed that microscopic flow details can be ignored, such as the dynamics of a single air bubble. However, as we have shown, the phenomenon of air entrainment can be an important feature of the physics. It is clearly not possible to model the production and collapse of each microscopic air bubble over the size of domain needed for WEC simulation, even if bubble physics was completely understood, so some form of integral fluid mixture model is used in the belief that enough of the essential physics will be captured and the material properties of the aerated fluid will be faithfully replicated. In some WEC simulations there will be a need to include turbulence but there are limits to the accuracy and applicability

of turbulence models and there are many competing models of turbulence (eg, the k-epsilon model, the k-omega model, the Spalart–Allmaras model (Spalart and Allmaras, 1992) and the Re-Normalization Group k-epsilon model (Yakhot et al., 1992)), which itself is not completely understood and is highly problem dependent. Then there is the water. WECs operate in sea water but numerical models (and wave tank tests) currently use fresh water. Sea water can have quite different properties to fresh water depending on its temperature and salt content and this is a topic that does not seem to have been studied extensively. Finally, most numerical models assume that WECs are completely rigid when in fact they may deform appreciably in response to a large wave, so these models may need to be extended to include scenarios where structures are flexible and detailed calculations of extreme loads are required.

6.6 FUTURE DEVELOPMENTS

Significant advances have been made in CFD during the last few decades, which have also seen massive improvements in computer hardware, including massively parallel implementations. This has led to the development of a large number of independent CFD codes for fluid/structure interactions written in different languages and running on different systems. These codes possess elements which, if extracted and put together into a single code, could improve current WEC simulation. However, research codes are usually written in a piecemeal way, are poorly documented and are difficult for third parties to adapt to their particular needs. There is also the problem that some researchers have been reluctant to make their codes available to the wider community (even though they were funded from public research grants) and it is a very difficult and time consuming undertaking to rewrite code from scratch using the available published literature. We believe that the current situation is an impediment to progress in CFD modelling of WSI in general and WEC simulation in particular.

A potentially significant development is the creation of a repository of open-source code for generic WSI problems based around the OpenFoam software (<http://www.openfoam.com>). OpenFoam is a freely available open-source package which is becoming widely used in CFD and facilitates the development of custom-built open-source CFD NWT software for WSI problems, including for the modelling of WECs. OpenFoam contains a large number of models, advanced gridding routines and parallelization options. Furthermore, the source code is provided and the package is well structured, documented and comes with tutorial examples. The approach has been to take a fixed version of OpenFoam as a starting point and embed it into a dedicated software repository. In this way, as software is developed it is tested, documented,

structured and maintained to professional software engineering standards. Modules can be checked from the main branch of the repository, developed within the code developer's branch and checked back into the main repository subject to stringent code verification tests being passed. By adhering to the OpenFoam structure, it should be possible for the CFD community to make rapid advances by contributing to and making use of the latest innovations without having to constantly replicate code. We have thus developed OpenFoam modules to simulate the Oyster WEC as shown in Fig. 6.7. Work is currently being undertaken with partners to produce a more general OpenFoam framework for coupling different flow solvers such as full potential codes, CFD NWT codes and structural dynamics models to produce an efficient hybrid NWT code for wave structure interaction (WSI-Foam). Such a code will be freely available on the understanding that any developments are put back into the repository for the benefit of the CFD community.

Looking to the future, given the continuing advances being made in fluid dynamics models, numerical methods and computer architecture, the authors believe that eventually CFD could become the standard approach for WEC engineers.

6.7 SUMMARY

- CFD models involve solving the Navier–Stokes equation together with the continuity equation for particular initial and boundary conditions.
- CFD models can be Eulerian (grid-based) or Lagrangian (particle-based).
- Accuracy of the CFD model depends on ensuring that all of the relevant physics is included in the model.
- CFD numerical algorithms involve approximations that result in intrinsic errors and numerical dissipation.

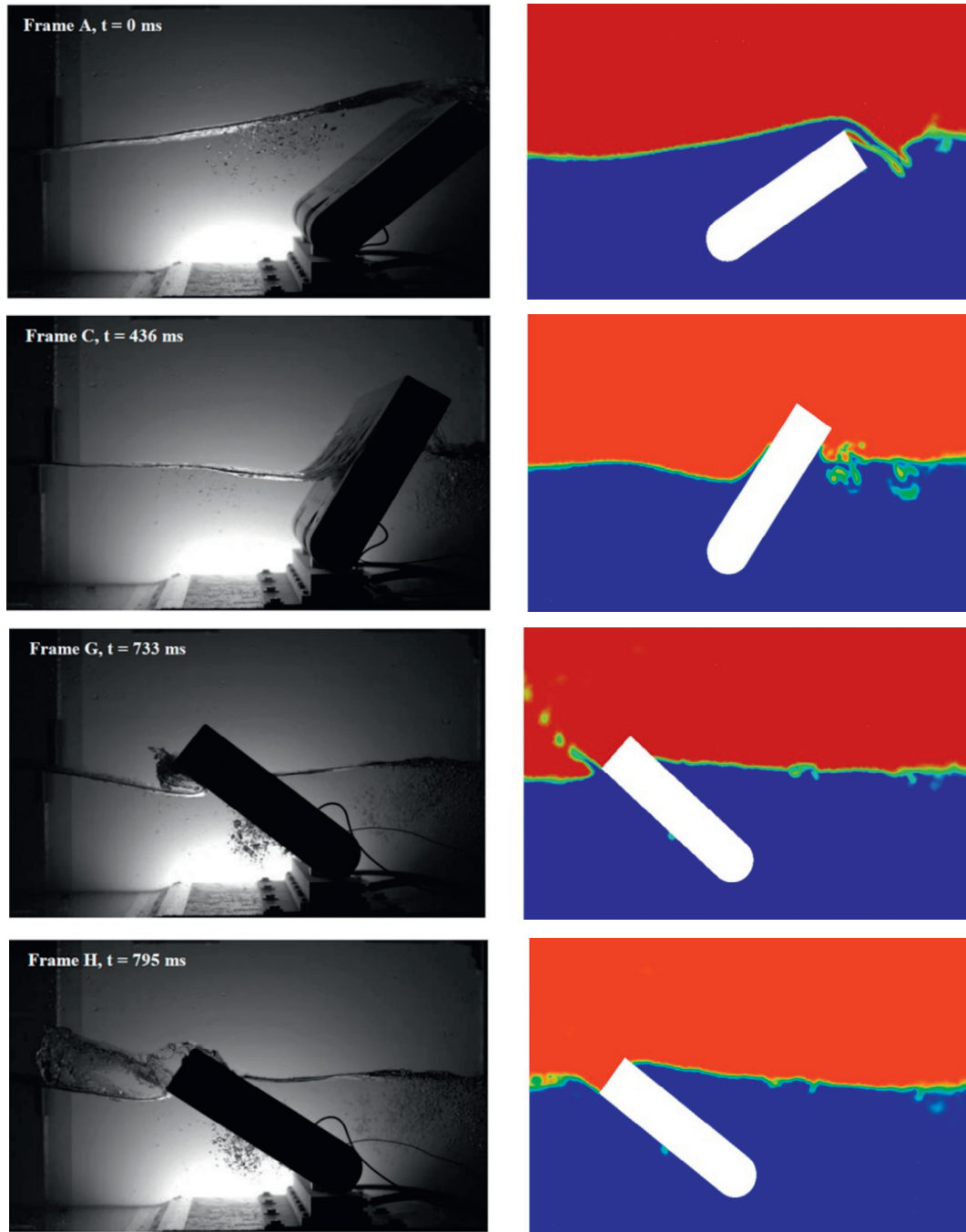


FIG. 6.7 OpenFoam simulation of an oscillating wave surge converter at various times using AMI gridding and the waves2Foam solver (2D). *Left*: experiments. *Right*: numerical simulation.

- A wide range of commercial and noncommercial CFD modelling packages are available; all of these have limitations and the choice should be driven by the important physics.
- It takes considerable experience and expertise to correctly set up and run a simulation.
- Large WEC motions can cause gridding issues either due to grid distortion or the requirement to remesh/interpolate grids.
- An incompressible CFD model may underestimate extreme loads.
- SPH models are emerging as suitable for model response/loads in extreme waves.
- Computational speed remains a significant limitation for CFD models.
- CFD modelling tools continue to be developed with OpenFoam potentially offering a framework for future collaboration.

References

- Agamloh, E.B., Wallace, A.K., Von Jouanne, A., 2008. Application of fluid–structure interaction simulation of an ocean wave energy extraction device. *Renew. Energy* 33, 748–757.
- Alves, M., Sarmento, A., 2006. Non-linear and viscous analysis of the diffraction flow in OWC wave power plants. In: 16th International Offshore and Polar Engineering Conference, San Francisco, USA, pp. 179–184.
- Anbarsooz, M., Passandideh-Fard, M., Moghiman, M., 2014. Numerical simulation of a submerged cylindrical wave energy converter. *Renew. Energy* 64, 132–143.
- Babarit, A., Mouslim, H., Clement, A., et al., 2009. On the numerical modelling of the non linear behaviour of a wave energy converter. In: 28th International Conference on Ocean, Offshore and Arctic Engineering, Honolulu, USA, pp. 1045–1053.
- Bhinder, M.A., Mingham, C.G., Causon, D.M., Rahmati, M.T., Aggidis, G.A., Chaplin, R.V., 2009. A joint numerical and experimental study of a surging point absorbing wave energy converter (WRASPA). In: ASME 28th Int. Conf. on Ocean, Offshore and Arctic Engineering.
- Bhinder, M.A., Babarit, A., Gentaz, L., et al., 2011. Assessment of viscous damping via 3D-CFD modelling of a floating wave energy device. In: 9th European Wave and Tidal Energy Conference, Southampton, UK.
- Causon, D.M., Mingham, C.G., 2010. *Introductory Finite Difference Methods for PDEs*. Ventus Publishing ApS. ISBN: 978-87-7681-642-1.
- Causon, D.M., Ingram, D.M., Mingham, C.G., 2001. A Cartesian cut cell method for shallow water flows with moving boundaries. *Adv. Water Resour.* 24 (8), 899–911.
- Causon, D.M., Mingham, C.G., Qian, L., 2011. *Introductory Finite Volume Methods for PDEs*. Ventus Publishing ApS. ISBN: 978-87-7681-882-1.
- Drazin, P.G., Riley, N., 2006. *The Navier–Stokes Equations: A Classification of Flows and Exact Solutions*. Cambridge University Press, Cambridge. ISBN-13: 978-0521681629.
- Henry, A., Rafiee, A., Schmitt, P., Dias, F., Whittaker, T., 2014. The characteristics of wave impacts on an oscillating wave surge converter. *J. Ocean Wind Energy* 1 (2), 101–110.
- Hu, Z.Z., Causon, D.M., Mingham, C.G., Qian, L., 2011. Numerical simulation of floating bodies in extreme free surface waves. *Nat. Hazards Earth Syst. Sci.* 11 (2), 519–527.
- Leveque, R.J., 2007. *Finite Difference Methods for Ordinary and Partial Differential Equations: Steady-State and Time-Dependent Problems*. SIAM, Philadelphia, PA. ISBN-13: 978-0898716290.
- Luo, Y., Nader, J.R., Cooper, P., et al., 2014. Nonlinear 2D analysis of the efficiency of fixed oscillating water column wave energy converters. *Renew. Energy* 64, 255–265.
- Ma, Z.H., Causon, D.M., Qian, L., Mingham, C.G., Gu, H.B., Martinez-Ferrer, P., 2014. A compressible multiphase flow model for violent aerated wave impact problems. *Proc. R. Soc. A* 470, 20140542.
- Monaghan, J.J., 2012. Smoothed particle hydrodynamics and its diverse applications. *Annu. Rev. Fluid Mech.* 44, 323–346.
- Omidvar, P., Stansby, P.K., Rogers, B.D., 2012. SPH for 3D floating bodies using variable mass particle distribution. *Int. J. Numer. Methods Fluids* 72, 427–452.
- Palm, J., Eskilsson, C., et al., 2013. CFD simulation of a moored floating wave energy converter. In: 10th European Wave and Tidal Energy Conference, Aalborg, Denmark.
- Qian, L., Mingham, C.G., Causon, D.M., Ingram, D.M., Folley, M., Whittaker, T.J.T., 2005. Numerical simulation of wave power devices using a two-fluid free surface solver. *Mod. Phys. Lett. B* 19 (28&29), 1479–1482.
- Qian, L., Causon, D.M., Mingham, C.G., Ingram, D.M., 2006. A free-surface capturing method for two fluid flows with moving bodies. *Proc. R. Soc. A* 462 (2065), 21–42.
- Rafiee, A., Elsaesser, B., Dias, F., 2013. Numerical simulations of wave interaction with an oscillating wave surge converter. In: 32nd International Conference on Ocean, Offshore and Arctic Engineering, Nantes, France.

- Schmitt, P., Elsaesser, B., 2015. On the use of OpenFOAM to model Oscillating Wave Surge Converters. *Ocean Eng.* 108, 98–104.
- Schmitt, P., Whittaker, T., Clabby, D., Doherty, K., 2012. The opportunities and limitations of using CFD in the development of wave energy converters. In: *Marine & Offshore Renewable Energy Conference*, London, UK, pp. 89–97.
- Spalart, P.R., Allmaras, S.R., 1992. A One-Equation Turbulence Model for Aerodynamic Flows. AIAA Paper 92-0439, the AIAA 30th Aerospace Sciences Meeting and Exhibition, 6–9 January, Reno, NV, USA.
- Thilleul, O., Baudry, V., Guilcher, P.M., Jacquin, E., Babarit, A., et al., 2011. Assessment of sizing parameters of a wave energy converter through the complementary use of a linear potential code, a RANS and a SPH solver. In: *9th European Wave and Tidal Energy Conference*, 2011, Southampton, United Kingdom.
- Ubbink, O., 1997. Numerical prediction of two fluid systems with sharp interfaces. (Ph.D. Thesis) Imperial College of Science, Technology and Medicine, London.
- Versteeg, H., Malalasekera, W., 2007. *An Introduction to Computational Fluid Dynamics: The Finite Volume Method*. Prentice Hall, Harlow, Essex, England. ISBN-13: 978-0131274983.
- Westphalen, J., Greaves, D.M., Williams, C.J.K., Taylor, P.H., Causon, D.M., Mingham, C.G., Hu, Z.Z., Stansby, P.K., Rogers, B.D., Omidvar, P., 2009. Extreme wave loading on offshore wave energy devices using CFD: a hierarchical team approach. In: *Proceedings 8th European Wave and Tidal Energy Conference (EWTEC)*, Uppsala, Sweden, pp. 501–508.
- Wolgamot, H., Fitzgerald, C., 2015. Nonlinear hydrodynamic and real fluid effects on wave energy converters. *Proc. IMechE A: J. Power Energy* 25 (1), 1–23.
- Yakhot, V., Orszag, S.A., Thangam, S., Gatski, T.B., Speziale, C.G., 1992. Development of turbulence models for shear flows by a double expansion technique. *Phys. Fluids A* 4 (7), 1510–1520.
- Yang, G., Causon, D.M., Ingram, D.M., 2000. Calculation of compressible flows about complex moving geometries using a 3D Cartesian cut cell method. *Int. J. Numer. Methods Fluids* 33, 1121–1151.
- Yu, Y.H., Li, Y., 2013. Reynolds-averaged Navier–Stokes simulation of the heave performance of a two-body floating-point absorber wave energy system. *Comput. Fluids* 73, 104–114.
- Zhang, Y., Zou, Q.P., Greaves, D., 2012. Air–water two-phase flow modelling of hydrodynamic performance of an oscillating water column device. *Renew. Energy* 41, 159–170.